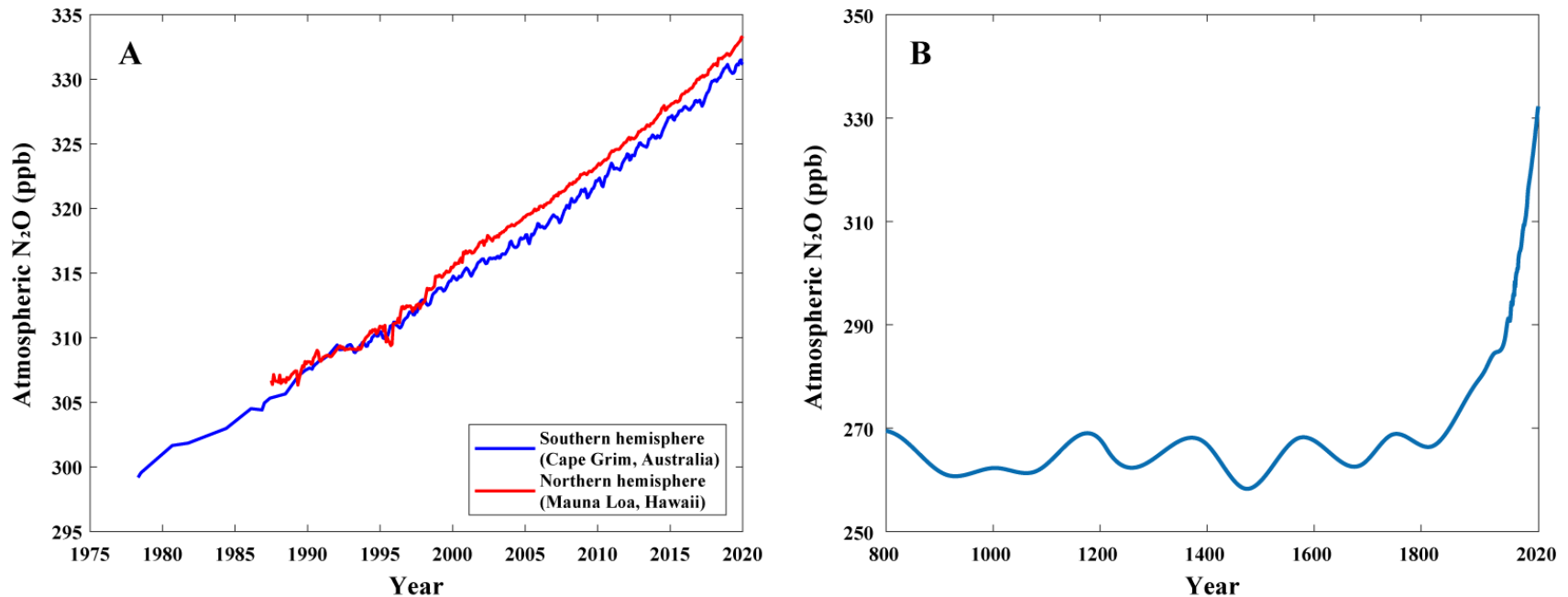
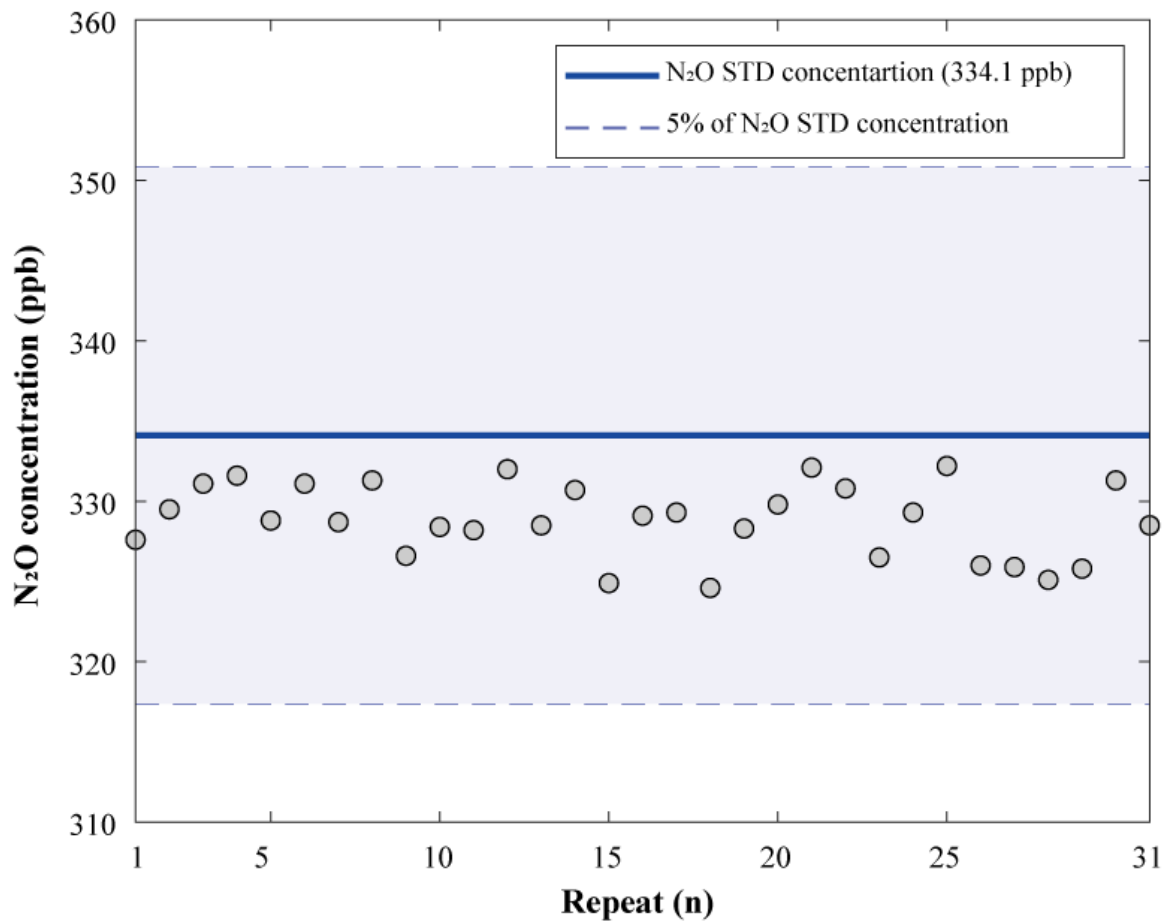


## Supporting Information



**Figure S1.** (A) Comparison of atmospheric N<sub>2</sub>O concentrations in the Northern and Southern Hemispheres. From 1987 to 2020, the mean difference in N<sub>2</sub>O concentration between the two locations was  $1.13 \pm 0.63$  ppb. (B) The line chart depicts the history of interpolated atmospheric N<sub>2</sub>O levels. The sources of the dataset are given in section 2.2.



**Figure S2.** N<sub>2</sub>O standard gas measurements (gray circles). Blue solid line represents a certified value of standard gas as 334.1 ppb. Dotted lines represent ±5 % levels of the certified value.

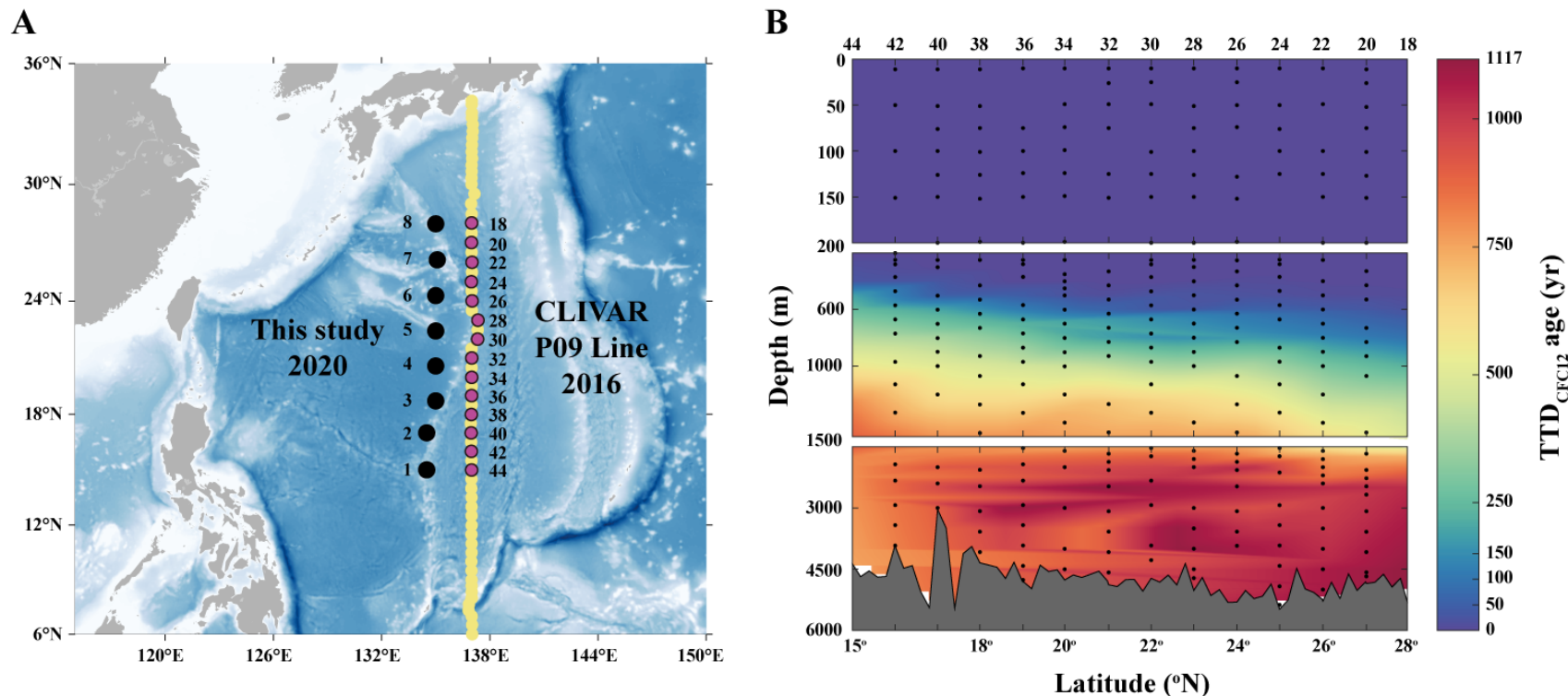


**Figure S3.** The map of the study area, CLIVAR P09 cruise (2016), and the vertical distribution of TTD<sub>CFC12</sub> age during the CLIVAR P09 cruise. **(A)** Black dots represent stations where sampling for this study was carried out, and yellow/purple dots indicate the sampling stations of the P09 cruise. The CFCs data set was obtained from CLIVAR stations colored in purple. **(B)** The vertical distribution of TTD<sub>CFC12</sub> age is colored with blue to red gradients. Black dots represent sampling depth, and the upper part of the *x*-axis represents station numbers of the P09 cruise.

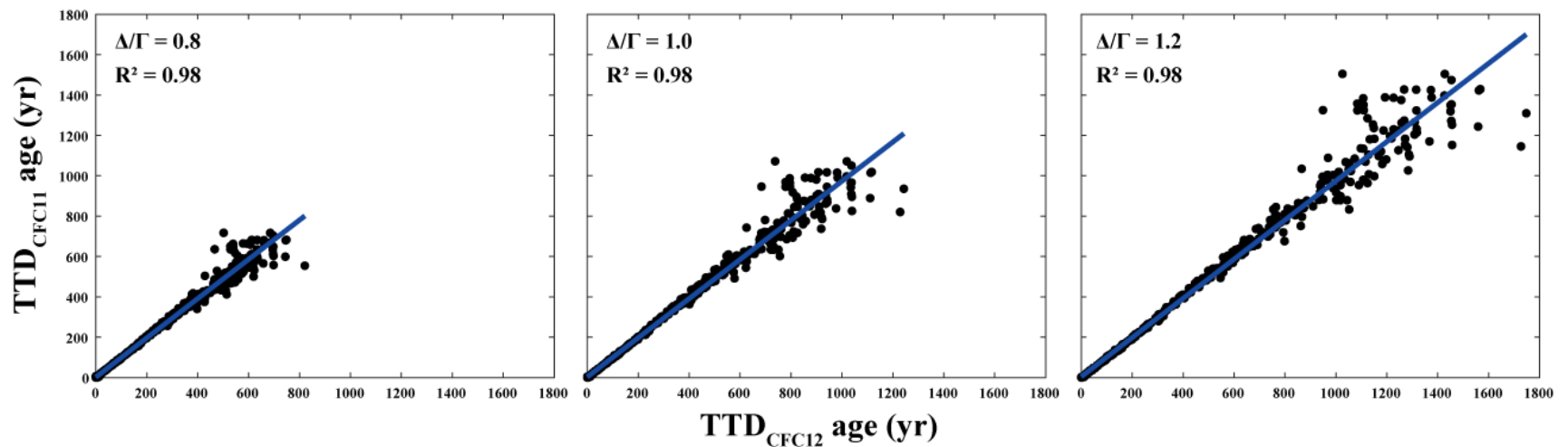


**Figure S4.** The correlations between  $\text{TTD}_{\text{CFC11}}$  and  $\text{TTD}_{\text{CFC12}}$  ages along three  $\Delta/\Gamma$  ratios (0.8, 1.0, and 1.2). The solid lines represent the 1:1 regression line.

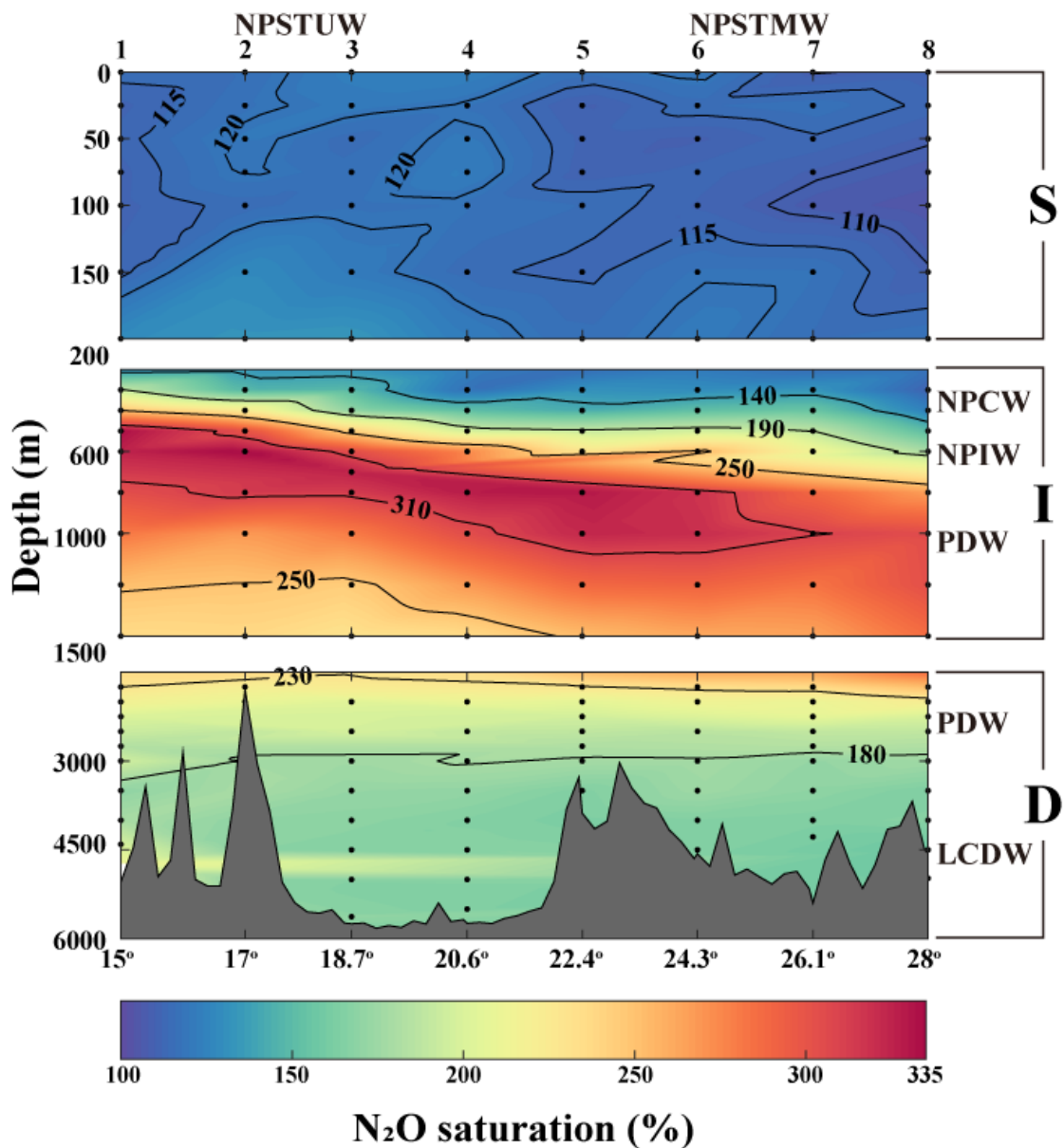


**Figure S5.** Vertical profiling of  $\text{N}_2\text{O}$  saturation in different layers: surface (0–200 m), intermediate (200–1500 m), and deep layers (1500–5774 m) of the STWNPO during this investigation. The black solid lines represent the contour lines and the abbreviations of water masses indicate the distribution of water masses. The top and bottom of the  $x$ -axis represent the station numbers and latitudes, respectively.

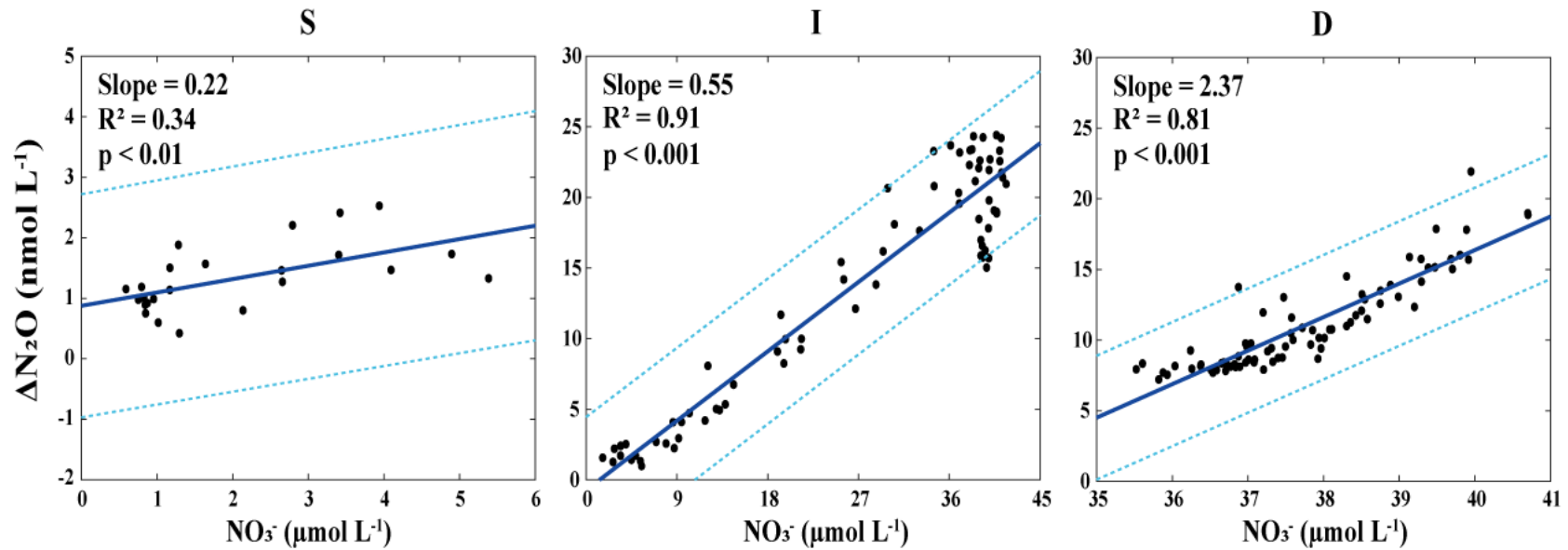


**Figure S6.** The correlations of  $\Delta\text{N}_2\text{O}$  with  $\text{NO}_3^-$  in each layer (surface, intermediate, and deep) of the STWNPO. The blue and cyan lines represent the linear regression and the 95% prediction interval respectively.

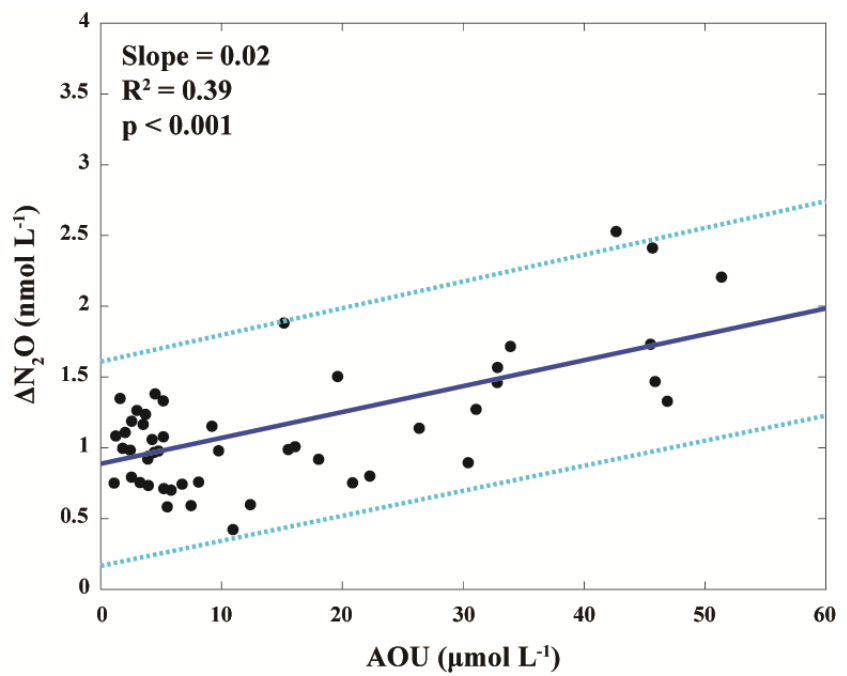


**Figure S7.** Correlations of  $\Delta\text{N}_2\text{O}$  with AOU at the surface layer (0–200 m). The blue and cyan lines represents the linear regression and the 95% prediction interval respectively.

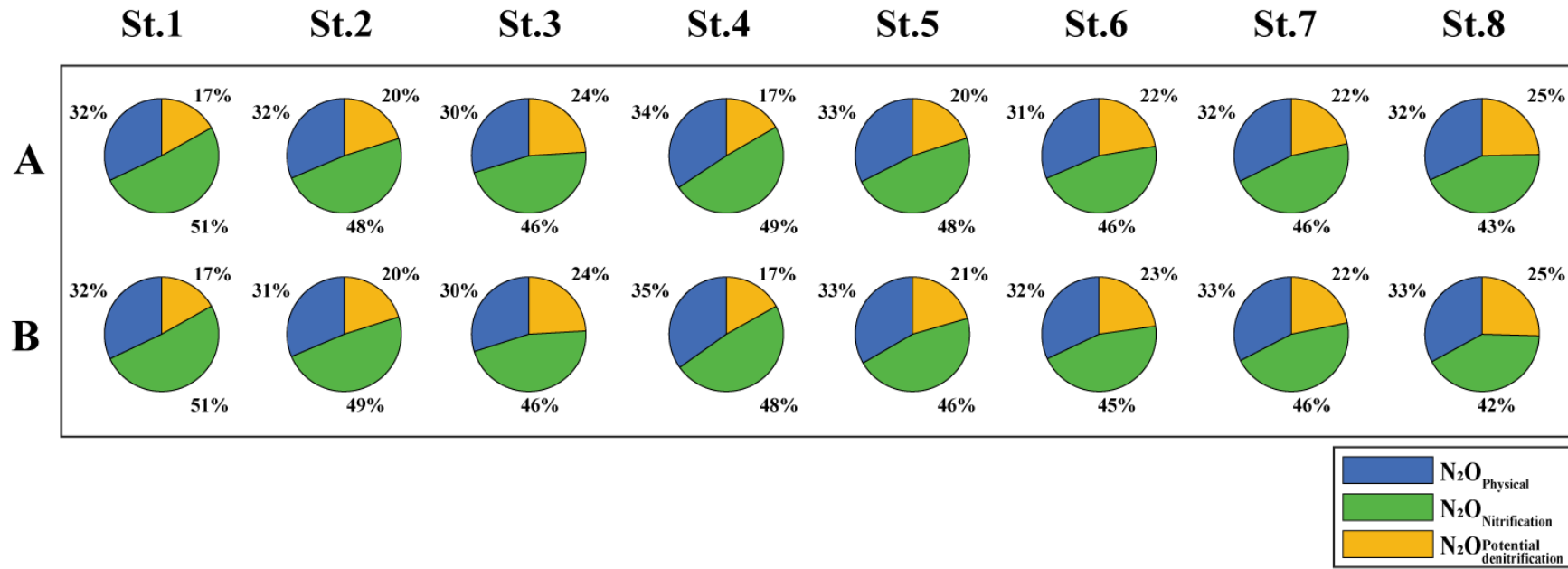


**Figure S8.** The estimated mean fractions of  $\text{N}_2\text{O}$  production derived from physical ( $\text{N}_2\text{O}_{\text{eq}}$ ) and biogeochemical ( $\text{N}_2\text{O}_{\text{Nitrification}}$  and  $\text{N}_2\text{O}_{\text{denitrification}}$ ) processes in the intermediate layer of the STWNPO during this study.  $\text{N}_2\text{O}_{\text{Nitrification}}$  was estimated using the slope of  $\Delta\text{N}_2\text{O}/\text{AOU}$  (**A**) and  $\Delta\text{N}_2\text{O}/\text{NO}_3^-$  (**B**). Given the error of  $r_{\Delta\text{N}_2\text{O}:\text{NO}_3^-}$ , the error for estimating  $\text{N}_2\text{O}_{\text{Nitrification}}$  was  $\pm 1.8\%$ .

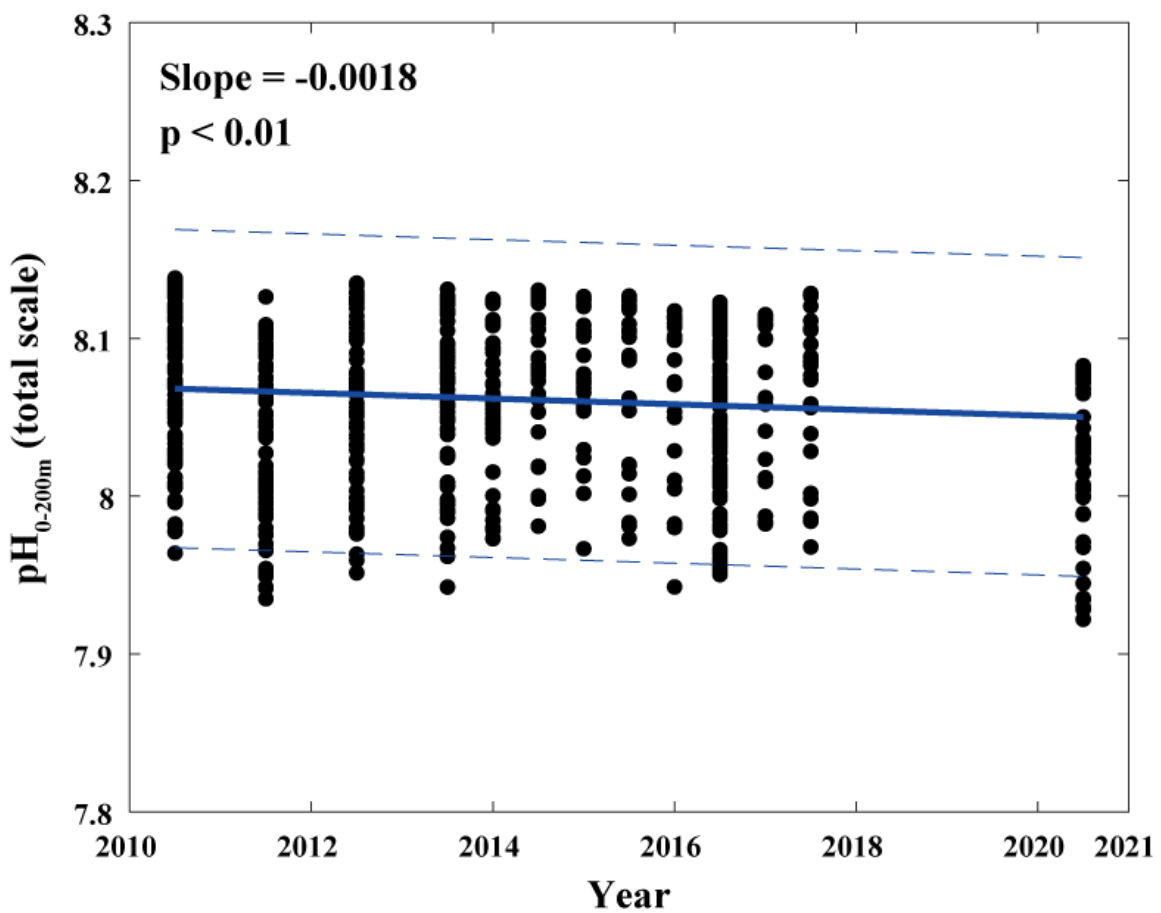


**Figure S9.** The temporal pH trend in the surface layer (0–200 m) of the STWNPO. The historic data were obtained from the stations indicated on the CLIVAR P09 transect line (refer to purple dots in Supplementary Fig. S3). The decreasing rate of surface pH was  $-0.0018 \text{ yr}^{-1}$  ( $p < 0.01$ ).

**Table S1.** The  $\Delta/\Gamma$  ratio in various environments.

Region	$\Delta/\Gamma$ Ratio	Tracer	References
Global	1	CFC12	Waugh et al. (2006)
North Atlantic (Subpolar)	1	CFCs, tritium, helium	Waugh et al. (2004)
Arctic, Nordic Seas, North Atlantic	0.8		
North Pacific, Southern Ocean	1.2	CFCs, SF6	He et al. (2018)
elsewhere	1		
North pacific (directly ventilated)	<1.0		
North pacific (ventilated by physical mixing)	>1.0	CFC11, SF6	Sonnerup et al. (2013)
Nordic Seas	0.5~1.5 (probable 1.0)	CFC11, CFC12	Olsen et al. (2010)
Northern South China Sea, Western North Pacific	0.8	CFC12, SF6	Wang et al. (2021)
Indian Ocean	1	CFC11, CFC12	Alvarez et al. (2009)
Global	1	CFC12, SF6	Shao et al. (2016)
South Pacific	0.6	CFC11, CFC12, SF6	Kim et al. (2013)

**Table S2.** The ranges and averages of excess N<sub>2</sub>O differences from the TTD<sub>CFC12</sub> ages of three  $\Delta/\Gamma$  ratios (i.e., 0.8, 1.0, and 1.2 [ $\Delta N_2O_{0.8}$ ,  $\Delta N_2O_{1.0}$ , and  $\Delta N_2O_{1.2}$ ]) and unmodified excess N<sub>2</sub>O ( $\Delta N_2O_{\text{Unmodified}}$ ).

Station	$\Delta N_2O_{1.0}-\Delta N_2O_{0.8}$	$\Delta N_2O_{1.0}-\Delta N_2O_{1.2}$	$\Delta N_2O_{1.0}-\Delta N_2O_{\text{Unmodified}}$
	(nmol L <sup>-1</sup> )		
1	-0.17 – 0.13 (0.06 ± 0.05)	-0.13 – 0.19 (0.05 ± 0.05)	0 – 2.43 (1.43 ± 1.11)
2	-0.17 – 0.28 (0.06 ± 0.07)	-0.24 – 0.17 (0.08 ± 0.08)	-0.26 – 2.39 (1.35 ± 1.11)
3	-0.18 – 0.26 (0.06 ± 0.07)	-0.40 – 0.14 (0.12 ± 0.12)	-0.34 – 2.40 (1.27 ± 1.10)
4	-0.17 – 0.18 (0.05 ± 0.06)	-0.39 – 0.07 (0.08 ± 0.10)	-0.30 – 2.47 (1.26 ± 1.15)
5	-0.18 – 0.37 (0.08 ± 0.09)	-0.40 – 0.33 (0.12 ± 0.15)	-0.30 – 2.46 (1.25 ± 1.15)
6	-0.08 – 0.31 (0.09 ± 0.09)	-0.39 – 0.10 (0.08 ± 0.11)	-0.26 – 2.37 (1.23 ± 1.12)
7	-0.08 – 0.23 (0.07 ± 0.07)	-0.24 – 0.19 (0.07 ± 0.08)	-0.28 – 2.50 (1.26 ± 1.19)
8	-0.19 – 0.20 (0.07 ± 0.08)	-0.40 – 0.06 (0.12 ± 0.15)	-0.26 – 2.47 (1.18 ± 1.15)
Mean	0.07 ± 0.07	0.09 ± 0.11	1.28 ± 1.12

**Table S3.** The water masses identified during this study. The values in parentheses are the values observed in this study.  $\theta$ , S, and  $\sigma_\theta$  refer to potential temperature, salinity, and potential density anomaly, respectively.

Water Mass	$\theta$ (°C)	S (psu)	$\sigma_\theta$ (kg m <sup>-3</sup> )	Layer	Characteristics	References
NPSTMW	16 – 20	34.6 – 34.8	25.0 – 25.6	Surface	Relatively high DO (~205.71 μmol L <sup>-1</sup> )	Hanawa and Talley (2001) Oka (2009) Rainville et al. (2014)
NPSTUW	19 – 25	34.6 – 35.4	23.0 – 25.0	Surface	Relatively low DO (~195.11 μmol L <sup>-1</sup> )	Suga et al. (2000) O'Connor et al. (2002) Behrens et al. (2018)
NPCW	10 – 22	34.2 – 35.2	25.2 – 26.4	Intermediate	Total alkalinity Minimum	Emery (2001) Behrens et al. (2018)
NPIW	5 – 12	34.0 – 34.3	26.6 – 27.4	Intermediate	Salinity Minimum (~34.15 psu)	Talley (1993) Behrens et al. (2018)
PDW	1.4 – 6.4	33.4 – 34.7	27.6 – 27.8	Deep	Oxygen Minimum (~55 μmol L <sup>-1</sup> ), Nutrient Maximum (NO <sub>3</sub> <sup>-</sup> : ~41.6 μmol L <sup>-1</sup> ), N* Minimum (-7.3 μmol L <sup>-1</sup> )	Amakawa et al. (2009) Talley (2011) Behrens et al. (2018)
LCDW	0.98 – 1.2	34.6 – 37.4	27.7 – 28.2	Deep	Low Silicate, High Salinity (~34.68 psu)	Emery (2001) Talley (2011)

**Table S4.** The slopes of  $\Delta\text{N}_2\text{O}/\text{AOU}$  and  $\Delta\text{N}_2\text{O}/\text{NO}_3^-$  in various ocean environments.

Region	Slope $_{\Delta\text{N}_2\text{O}/\text{AOU}}$ (mol N <sub>2</sub> O/mol O <sub>2</sub> )	Slope $_{\Delta\text{N}_2\text{O}/\text{NO}_3^-}$ (mol N <sub>2</sub> O/mol NO <sub>3</sub> <sup>-</sup> )	Depth (m)	References
Western Pacific, Indian Ocean	0.125 + 0.00993T	—	0 – 5900	Butler et al. (1989)
Tropical Atlantic	0.121 (central) 0.106 (eastern)	—	< 300	Forster et al. (2009)
Eastern Tropical South Pacific (O <sub>2</sub> > 50 μM)	0.13	—	< 350	Kock et al. (2016)
Eastern Tropical Pacific, Arabian Sea	0.2 – 0.3	—	σ <sub>θ</sub> = 26.9	
South Atlantic, South Indian	0.01 – 0.05	—	σ <sub>θ</sub> = 26.9	
Indian Ocean (0–5°N)	>0.22	—	200 – 300	Nevison et al. (2003)
Western Pacific (0–10°N)	>0.22	—	300	
Atlantic (20°N)	>0.14	—	300	
	0.0473 (subtropical)	0.2497	< 1000	
North Atlantic	0.0785 (tropical) 0.0942 (tropical)	0.4848 0.7379	< 500 > 500	Walter et al. (2006)
Western Arctic Ocean	0.039	0.22	75 – 150	Zhang et al. (2015)
South Pacific Subtropical Gyre	0.176 (central) 0.142 (eastern)	0.403 (AOU/NO <sub>3</sub> <sup>-</sup> ) 0.188 (AOU/NO <sub>3</sub> <sup>-</sup> )	200 – 600	Charpentier et al. (2007)
Gulf of Mexico	0.048, 0.096	—	0 – 32	Walker et al. (2010)
East China Sea, South Yellow Sea	0.0015 – 0.12	0.021 – 1.16	0 – 800	Chen et al. (2021)
	0.02	0.22	0 – 200	
Western North Pacific	0.09	0.55	200 – 1500	This study
	0.16	2.37	1500 – 5774	

**Table S5.** The slopes of  $\Delta\text{N}_2\text{O}/\text{AOU}$  and  $\Delta\text{N}_2\text{O}/\text{N}^*$  of the intermediate layer, NPIW, and PDW in the deep layer

	$\Delta\text{N}_2\text{O}/\text{AOU}$		$\Delta\text{N}_2\text{O}/\text{N}^*$	
	Slope	p value	Slope	p value
<b>Intermediate layer</b>	0.09	< 0.001	-2.32	< 0.001
<b>NPIW</b>	0.11	< 0.001	-1.35	< 0.05
<b>PDW in deep layer</b>	0.16	< 0.001	-0.84	< 0.001

**Table S6.** Observed wind speeds at the height of 29 m ( $U_{29}$ ) and estimated wind speeds at the height of 10 m ( $U_{10}$ ) during this investigation.

Station	Year	Month	Date	Time	Observed $U_{29}$ ( $\text{m s}^{-1}$ )	Estimated $U_{10}$ ( $\text{m s}^{-1}$ )
1	2020	5	27	13:13 – 13:43	6.72	6.15
2	2020	5	30	15:28 – 15:58	5.51	5.04
3	2020	5	31	08:53 – 09:23	4.74	4.34
4	2020	6	1	00:43 – 01:13	5.38	4.92
5	2020	6	2	00:53 – 01:23	3.85	3.52
6	2020	6	2	19:10 – 19:40	6.94	6.36
7	2020	6	3	11:45 – 12:15	7.27	6.65
8	2020	6	4	08:44 – 09:14	13.59	12.44

**Table S7.** Estimated N<sub>2</sub>O fluxes using three  $k_w$  models during this investigation of the STWNPO. W&M<sub>1999</sub>, N<sub>2000</sub>, and W<sub>2014</sub> refer to the kw models of Wanninkhof and McGillis (1999), Nightingale et al. (2000), and Wanninkhof (2014), respectively.

Station	N <sub>2</sub> O Flux ( $\mu\text{mol m}^{-2} \text{d}^{-1}$ )				
	W&M <sub>1999</sub>	N <sub>2000</sub>	W <sub>2014</sub>	Mean	STD
1	1.3	2.0	1.9	1.8	0.4
2	0.8	1.5	1.4	1.2	0.4
3	0.7	1.7	1.5	1.3	0.5
4	1.2	2.3	2.1	1.8	0.6
5	0.3	0.8	0.7	0.6	0.3
6	2.1	3.0	2.9	2.7	0.5
7	0.8	1.0	1.0	0.9	0.2
8	7.1	4.8	5.1	5.6	1.3
<b>Mean</b>			2.0	0.3	

**Table S8.** N<sub>2</sub>O fluxes of various regions.

Region	N <sub>2</sub> O <sub>Flux</sub> (μmol m <sup>-2</sup> d <sup>-1</sup> )	References
<b>Pacific</b>		
East China Sea	6.9 – 7.0	Zhang et al. (2019)
Northeastern coast of Australia	-0.2 ± 0.1	Reading et al. (2021)
Yellow Sea	0.2 – 7.7	Chen et al. (2021)
Okhotsk Sea	~2.5	Zhan et al. (2021)
Northeast subarctic Pacific	~12.5 12.7 – 30.7	Fenwick and Tortell (2018) Farías et al. (2009)
Eastern tropical South Pacific	27 – 1825 23 – 108	Arevalo-Martínez et al. (2015) Ji et al. (2019)
Subtropical North Pacific (Hawaii)	< 0.4 ± 0.2 0.04 – 0.13	Dore et al. (1998) Butler et al. (1989)
Western North Pacific (subtropical)	0.7 – 0.9 ~0.5 0.3 – 7.1	Breider et al. (2015) Yoshikawa et al. (2016) This Study
Western North Pacific (subarctic)	1.3 – 2.4 ~6.3	Breider et al. (2015) Yoshikawa et al. (2016)
<b>Indian</b>		
Indian Shelf	-1.2 – 3243	Naqvi et al. (2006)
<b>Atlantic</b>		
Nordic Sea	-4.4 ± 0.4	Zhan et al. (2016)
Southern Iberian Atlantic Basin	3.6 ± 13.7	Sierra et al. (2020)
Eastern subtropical South Atlantic	52.7 ± 43.2 ~46	Morgan et al. (2019) Frame et al. (2014)
Gulf of Mexico	3.2 – 5.2	Walker et al. (2010)
<b>Black Sea</b>		
Northwest shelf	1.6 – 4.4	Amouroux et al. (2002)
Deep basin	3.1 – 5.2	
<b>Arctic</b>		
Southern Chukchi Sea	2.3 ± 2.7	Heo et al. (2021)
Northern Chukchi Sea	-1.3 ± 1.5	
<b>Antarctic</b>		
Antarctic peninsula	-3.65 ± 0.95	Zhan et al. (2015)

## References

- Alvarez, M., Monaco, C.L., Tanhua, T., Yool, A., Oschlies, A., Bullister, J.L., et al. (2009). Estimating the storage of anthropogenic carbon in the subtropical Indian Ocean: a comparison of five different approaches. *Biogeosciences* 6(4), 681-703. doi: 10.5194/bg-6-681-2009.
- Amakawa, H., Sasaki, K., and Ebihara, M. (2009). Nd isotopic composition in the central North Pacific. *Geochimica et Cosmochimica Acta* 73(16), 4705-4719. doi: 10.1016/j.gca.2009.05.058.
- Amouroux, D., Roberts, G., Rapsomanikis, S., and Andreae, M. (2002). Biogenic gas ( $\text{CH}_4$ ,  $\text{N}_2\text{O}$ , DMS) emission to the atmosphere from near-shore and shelf waters of the north-western Black Sea. *Estuarine, Coastal and Shelf Science* 54(3), 575-587. doi: 10.1006/ecss.2000.0666.
- Arevalo-Martínez, D.L., Kock, A., Löscher, C., Schmitz, R.A., and Bange, H.W. (2015). Massive nitrous oxide emissions from the tropical South Pacific Ocean. *Nature Geoscience* 8(7), 530-533. doi: 10.1038/ngeo2469.
- Behrens, M.K., Pahnke, K., Schnetger, B., and Brumsack, H.-J. (2018). Sources and processes affecting the distribution of dissolved Nd isotopes and concentrations in the West Pacific. *Geochimica et Cosmochimica Acta* 222, 508-534. doi: 10.1016/j.gca.2017.11.008.
- Breider, F., Yoshikawa, C., Abe, H., Toyoda, S., and Yoshida, N. (2015). Origin and fluxes of nitrous oxide along a latitudinal transect in western North Pacific: Controls and regional significance. *Global Biogeochemical Cycles* 29(7), 1014-1027. doi: 10.1002/2014GB004977.
- Butler, J.H., Elkins, J.W., Thompson, T.M., and Egan, K.B. (1989). Tropospheric and dissolved  $\text{N}_2\text{O}$  of the west Pacific and east Indian Oceans during the El Niño Southern Oscillation event of 1987. *Journal of Geophysical Research: Atmospheres* 94(D12), 14865-14877. doi: 10.1029/JD094iD12p14865.
- Charpentier, J., Farias, L., Yoshida, N., Boontanon, N., and Raimbault, P. (2007). Nitrous oxide distribution and its origin in the central and eastern South Pacific Subtropical Gyre. *Biogeosciences* 4(5), 729-741. doi: 10.5194/bg-4-729-2007.
- Chen, X., Ma, X., Gu, X., Liu, S., Song, G., Jin, H., et al. (2021). Seasonal and spatial variations of  $\text{N}_2\text{O}$  distribution and emission in the East China Sea and South Yellow Sea. *Science of The Total Environment* 775, 145715. doi: 10.1016/j.scitotenv.2021.145715.
- Dore, J.E., Popp, B.N., Karl, D.M., and Sansone, F.J. (1998). A large source of atmospheric nitrous oxide from subtropical North Pacific surface waters. *Nature* 396(6706), 63-66. doi: 10.1038/23921.
- Emery, W.J. (2001). "Water types and water masses," in *Encyclopedia of ocean sciences (Second Edition)*. Academic Press, 291-299.
- Farías, L., Castro-González, M., Cornejo, M., Charpentier, J., Faúndez, J., Boontanon, N., et al. (2009). Denitrification and nitrous oxide cycling within the upper oxycline of the eastern tropical South Pacific oxygen minimum zone. *Limnology and Oceanography* 54(1), 132-144. doi: 10.4319/lo.2009.54.1.0132.

- Fenwick, L., and Tortell, P.D. (2018). Methane and nitrous oxide distributions in coastal and open ocean waters of the Northeast Subarctic Pacific during 2015–2016. *Marine Chemistry* 200, 45-56. doi: 10.1016/j.marchem.2018.01.008.
- Forster, G., Upstill-Goddard, R.C., Gist, N., Robinson, C., Uher, G., and Woodward, E.M.S. (2009). Nitrous oxide and methane in the Atlantic Ocean between 50°N and 52°S: latitudinal distribution and sea-to-air flux. *Deep Sea Research Part II: Topical Studies in Oceanography* 56(15), 964-976. doi: 10.1016/j.dsr2.2008.12.002.
- Frame, C.H., Deal, E., Nevison, C.D., and Casciotti, K.L. (2014). N<sub>2</sub>O production in the eastern South Atlantic: Analysis of N<sub>2</sub>O stable isotopic and concentration data. *Global Biogeochemical Cycles* 28(11), 1262-1278. doi: 10.1002/2013GB004790.
- Hanawa, K., and Talley, L.D. (2001). "Mode waters," in *International Geophysics*. Academic Press), 373-386.
- He, Y.C., Tjiputra, J., Langehaug, H.R., Jeansson, E., Gao, Y., Swinger, J., et al. (2018). A model-based evaluation of the inverse Gaussian transit-time distribution method for inferring anthropogenic carbon storage in the ocean. *Journal of Geophysical Research: Oceans* 123(3), 1777-1800. doi: 10.1002/2017JC013504.
- Heo, J.-M., Kim, S.-S., Kang, S.-H., Yang, E.J., Park, K.-T., Jung, J., et al. (2021). N<sub>2</sub>O dynamics in the western Arctic Ocean during the summer of 2017. *Scientific reports* 11(1), 1-12. doi: 10.1038/s41598-021-92009-1.
- Ji, Q., Altabet, M.A., Bange, H.W., Graco, M.I., Ma, X., Arévalo-Martínez, D.L., et al. (2019). Investigating the effect of El Niño on nitrous oxide distribution in the eastern tropical South Pacific. *Biogeosciences* 16(9), 2079-2093. doi: 10.5194/bg-16-2079-2019.
- Kim, I.N., Min, D.H., and Macdonald, A.M. (2013). Water column denitrification rates in the oxygen minimum layer of the Pacific Ocean along 32°S. *Global biogeochemical cycles* 27(3), 816-827. doi: 10.1002/gbc.20070.
- Kock, A., Arévalo-Martínez, D.L., Löscher, C.R., and Bange, H.W. (2016). Extreme N<sub>2</sub>O accumulation in the coastal oxygen minimum zone off Peru. *Biogeosciences* 13(3), 827-840. doi: 10.5194/bg-13-827-2016.
- Morgan, E.J., Lavric, J.V., Arévalo-Martínez, D.L., Bange, H.W., Steinhoff, T., Seifert, T., et al. (2019). Air-sea fluxes of greenhouse gases and oxygen in the northern Benguela Current region during upwelling events. *Biogeosciences* 16(20), 4065-4084. doi: 10.5194/bg-16-4065-2019.
- Nightingale, P.D., Malin, G., Law, C.S., Watson, A.J., Liss, P.S., Liddicoat, M.I., et al. (2000). In situ evaluation of air-sea gas exchange parameterizations using novel conservative and volatile tracers. *Global Biogeochemical Cycles* 14(1), 373-387. doi: 10.1029/1999GB900091.
- Naqvi, S.W.A., Naik, H., Jayakumar, D., Shailaja, M., and Narvekar, P. (2006). "Seasonal oxygen deficiency over the western continental shelf of India," in *Past and Present water column anoxia*. Springer), 195-224.
- Nevison, C., Butler, J.H., and Elkins, J. (2003). Global distribution of N<sub>2</sub>O and the ΔN<sub>2</sub>O-AOU yield in the subsurface ocean. *Global Biogeochemical Cycles* 17(4). doi: 10.1029/2003GB002068.
- O'Connor, B.M., Fine, R.A., Maillet, K.A., and Olson, D.B. (2002). Formation rates of subtropical underwater in the Pacific Ocean. *Deep Sea Research Part I:*

- Oceanographic Research Papers* 49(9), 1571-1590. doi: 10.1016/S0967-0637(02)00087-0.
- Oka, E. (2009). Seasonal and interannual variation of North Pacific subtropical mode water in 2003–2006. *Journal of oceanography* 65(2), 151-164. doi: 10.1007/s10872-009-0015-y.
- Olsen, A., Omar, A.M., Jeansson, E., Anderson, L.G., and Bellerby, R.G. (2010). Nordic seas transit time distributions and anthropogenic CO<sub>2</sub>. *Journal of Geophysical Research: Oceans* 115(C5). doi: 10.1029/2009JC005488.
- Rainville, L., Jayne, S.R., and Cronin, M.F. (2014). Variations of the North Pacific subtropical mode water from direct observations. *Journal of climate* 27(8), 2842-2860. doi: 10.1175/JCLI-D-13-00227.1.
- Reading, M.J., Maher, D.T., Santos, I.R., Jeffrey, L.C., Cyronak, T.J., McMahon, A., et al. (2021). Spatial Distribution of CO<sub>2</sub>, CH<sub>4</sub>, and N<sub>2</sub>O in the Great Barrier Reef Revealed Through High Resolution Sampling and Isotopic Analysis. *Geophysical Research Letters* 48(15), e2021GL092534. doi: 10.1029/2021GL092534.
- Shao, A.E., Mecking, S., Thompson, L., and Sonnerup, R.E. (2016). Evaluating the use of 1-D transit time distributions to infer the mean state and variability of oceanic ventilation. *Journal of Geophysical Research: Oceans* 121(9), 6650-6670. doi: 10.1002/2016JC011900.
- Sierra, A., Jiménez-López, D., Ortega, T., Gómez-Parra, A., and Forja, J. (2020). Factors controlling the variability and emissions of greenhouse gases (CO<sub>2</sub>, CH<sub>4</sub> and N<sub>2</sub>O) in three estuaries of the Southern Iberian Atlantic Basin during July 2017. *Marine Chemistry* 226, 103867. doi: 10.1016/j.marchem.2020.103867.
- Sonnerup, R.E., Mecking, S., and Bullister, J.L. (2013). Transit time distributions and oxygen utilization rates in the Northeast Pacific Ocean from chlorofluorocarbons and sulfur hexafluoride. *Deep Sea Research Part I: Oceanographic Research Papers* 72, 61-71. doi: 10.1016/j.dsr.2012.10.013.
- Suga, T., Kato, A., and Hanawa, K. (2000). North Pacific Tropical Water: Its climatology and temporal changes associated with the climate regime shift in the 1970s. *Progress in Oceanography* 47(2-4), 223-256. doi: 10.1016/S0079-6611(00)00037-9.
- Talley, L.D. (1993). Distribution and formation of North Pacific intermediate water. *Journal of Physical Oceanography* 23(3), 517-537. doi: 10.1175/1520-0485(1993)023<0517:DAFONP>2.0.CO;2.
- Talley, L.D. (2011). *Descriptive physical oceanography: an introduction*. Academic press.
- Walker, J.T., Stow, C.A., and Geron, C. (2010). Nitrous oxide emissions from the Gulf of Mexico hypoxic zone. *Environmental science & technology* 44(5), 1617-1623. doi: 10.1021/es902058t.
- Walter, S., Bange, H.W., Breitenbach, U., and Wallace, D.W. (2006). Nitrous oxide in the north Atlantic Ocean. *Biogeosciences* 3(4), 607-619. doi: 10.5194/bg-3-607-2006.
- Wang, W., Cai, M., Huang, P., Ke, H., Liu, M., Liu, L., et al. (2021). Transit time distributions and apparent oxygen utilization rates in northern South China Sea using chlorofluorocarbons and sulfur hexafluoride data. *Journal of Geophysical Research: Oceans* 126(8), e2021JC017535. doi: 10.1029/2021JC017535.

- Wanninkhof, R. (2014). Relationship between wind speed and gas exchange over the ocean revisited. *Limnology and Oceanography: Methods* 12(6), 351-362. doi: 10.4319/lom.2014.12.351.
- Wanninkhof, R., and McGillis, W.R. (1999). A cubic relationship between air-sea CO<sub>2</sub> exchange and wind speed. *Geophysical Research Letters* 26(13), 1889-1892. doi: 10.1029/1999GL900363.
- Waugh, D., Hall, T., McNeil, B., Key, R., and Matear, R. (2006). Anthropogenic CO<sub>2</sub> in the oceans estimated using transit time distributions. *Tellus B: Chemical and Physical Meteorology* 58(5), 376-389. doi: 10.1111/j.1600-0889.2006.00222.x.
- Waugh, D.W., Haine, T.W., and Hall, T.M. (2004). Transport times and anthropogenic carbon in the subpolar North Atlantic Ocean. *Deep Sea Research Part I: Oceanographic Research Papers* 51(11), 1475-1491. doi: 10.1016/j.dsr.2004.06.011.
- Yoshikawa, C., Abe, H., Aita, M.N., Breider, F., Kuzunuki, K., Toyoda, S., et al. (2016). Insight into nitrous oxide production processes in the western North Pacific based on a marine ecosystem isotopomer model. *Journal of Oceanography* 72(3), 491-508. doi: 10.1007/s10872-015-0308-2.
- Zhan, L., Chen, L., Zhang, J., Yan, J., Li, Y., and Wu, M. (2016). A permanent N<sub>2</sub>O sink in the Nordic Seas and its strength and possible variability over the past four decades. *Journal of Geophysical Research: Oceans* 121(8), 5608-5621. doi: 10.1002/2016JC011925.
- Zhan, L., Chen, L., Zhang, J., Yan, J., Li, Y., Wu, M., et al. (2015). Austral summer N<sub>2</sub>O sink and source characteristics and their impact factors in Prydz Bay, Antarctica. *Journal of Geophysical Research: Oceans* 120(8), 5836-5849. doi: 10.1002/2015JC010944.
- Zhan, L., Zhang, J., Ouyang, Z., Lei, R., Xu, S., Qi, D., et al. (2021). High-resolution distribution pattern of surface water nitrous oxide along a cruise track from the Okhotsk Sea to the western Arctic Ocean. *Limnology and Oceanography* 66(S1), S401-S410. doi: 10.1002/lno.11604.
- Zhang, G.L., Liu, S.M., Casciotti, K.L., Forbes, M.S., Gu, X.J., Ren, Y.Y., et al. (2019). Distribution of concentration and stable isotopic composition of N<sub>2</sub>O in the shelf and slope of the Northern South China Sea: implications for production and emission. *Journal of Geophysical Research: Oceans* 124(8), 6218-6234. doi: 10.1029/2019JC014947.
- Zhang, J., Zhan, L., Chen, L., Li, Y., and Chen, J. (2015). Coexistence of nitrous oxide undersaturation and oversaturation in the surface and subsurface of the western Arctic Ocean. *Journal of Geophysical Research: Oceans* 120(12), 8392-8401. doi: 10.1002/2015JC011245.